Seasonal and inter-annual rainfall patterns drive Mediterranean cork oak woodland carbon uptake and sequestration

Joana Boavida-Portugal[a,1,], Catarina F. Moura[c,d,2], Nuno Carvalhais[c,d], Mirco Migliavacca[c], Tarek S. El-Madany[c], João M. N. Silva[a], Rajchandar Padmanaban[a], Sofia Cerasoli[a] *

[a] Forest Research Centre, School of Agriculture, University of Lisbon, Tapada da Ajuda, 1349-017 Lisbon, Portugal

[1] Present address: MARE - Centro de Ciências do Mar e do Ambiente, Universidade de Évora, Largo dos Colegiais 2, 7004-516 Évora, Portugal

[c] Max Planck Institute for Biogeochemistry, Hans Knöll Straße 10, D-07745, Jena Germany

[d] Universidade Nova de Lisboa, Portugal

[2] Present address: Centre for Functional Ecology, Department of Life Sciences, University of Coimbra, Coimbra, Portugal

* corresponding author: sofiac@isa.ulisboa.pt (Sofia Cerasoli)

Abstract

Cork oak woodlands are low impact agroforestry ecosystems with high biodiversity and high social and economic value. Current climate change projections for the Mediterranean region foresee a decrease in the amount, and a change in the seasonality, of precipitation as well as an increase in temperature, threatening productivity and future carbon sequestration in these ecosystems. Analyses of long-term observations of both carbon fluxes and meteorological variables contribute to a better understanding of the ecosystem´s response to climate drivers and help predict its structural and functional stability under anticipated climate change.

In this study, we investigated the impact of rainfall variability on seasonal and inter-annual carbon sequestration in a Mediterranean cork oak woodland across seven hydrological years. Furthermore, the impact of rainfall and other climate variables on the start and end of the growing season of the understory was evaluated as well the sensitivity of carbon fluxes to the variability of the growing season length.

The site is a strong carbon sink with a mean annual Net Ecosystem Exchange (NEE) of about -338 ± 70 g C $m^{-2}y^{-1}$ turning into a weak carbon source only occasionally in autumn when rainfall is particularly low in the previous summer. We observed a time-lag effect of up to 12 months in the correlation between rainfall and NEE with the highest influence occurring at 6-month time-lag for all carbon fluxes. The length of the growing season of the understory vegetation depended on rainfall and vapor pressure deficit in periods preceding the start and end of the growing season but also on winter rainfall and explained about 70% of inter-annual variability of summer gross primary productivity (GPP) and ecosystem respiration (Reco).

Analyses of inter-annual and seasonal rainfall patterns, as well as of associated lagged effects on carbon dynamics, are not only relevant for our understanding of ecosystem functioning under future climate change but also for planning forest management actions that maximize carbon sequestration in Mediterranean oak woodlands .

Keywords: Mediterranean region; cork oak woodlands; CO_2 fluxes; eddy covariance; drought; precipitation

1. Introduction

Cork oak woodlands are low impact agroforestry ecosystems with high socio-economic and conservation value, widely distributed in the western Mediterranean region. They are characterized by a sparse tree cover of cork oak trees (*Quercus suber* L) and a diverse understory vegetation, ranging from shrub formations to grasslands (Bugalho et al., 2011). Portugal has the largest cork oak habitat worldwide representing 23% of the national forested area (ICNF, 2019). In addition to the economically important cork production and pasture, cork oak woodlands provide several ecosystem services, such as microclimate regulation, soil retention, air quality improvement, nutrient regulation, biodiversity conservation and carbon sequestration (Bugalho et al., 2011).

About 70% of Portuguese cork oak woodlands are concentrated in the southern part of the country (ICNF, 2019), a region characterized by a Mediterranean climate, with scarce water resources and a long dry summer season, usually coupled with high temperatures and high radiation (Faria et al., 1996). Climate change scenarios for the region anticipate increased vulnerability resulting from the combination of a decrease in annual precipitation, changes in precipitation seasonality and an increase in temperature (Dubrovský et al., 2014; Giorgi and Lionello, 2008). An increase in the intensity and frequency of extreme events is also expected (IPCC, 2021).

Trees and understory species characteristic of Mediterranean oak woodlands are well adapted to seasonally dry climate conditions typical of this region. However, the stability of these ecosystems under prolonged and exacerbated droughts is largely unknown and could compromise many of their ecological functions including their carbon sequestration capacity (Mori et al., 2017). Even though individually Mediterranean regions provide only a modest contribution to the overall biosphere-atmosphere carbon budget, as part of semi-arid ecosystems they contribute considerably to the degree of uncertainty in global CO_2 fluxes variability, thus hindering predictions of the global carbon cycle (Ahlström et al., 2015). This underlines the

75 importance of understanding the environmental controls on carbon exchange fluxes in these
76 regions.
77 A key feature to diagnose the complex responses of ecosystems to climate drivers has been the
78 analysis of carbon and water exchange between the ecosystem and the atmosphere. Eddy
79 covariance measurements provide time series of carbon and water fluxes and meteorological
80 variables largely contributing to the understanding of the biophysical and climate factors
81 determining the carbon exchange between the biosphere and the atmosphere from hourly to
82 multi-annual time scales (Baldocchi, 2020). Canopy-scale photosynthesis (gross primary
83 productivity; GPP) and ecosystem respiration (Reco) are the two processes determining the
84 magnitude of the net ecosystem CO_2 exchange (NEE) between the biosphere and the
85 atmosphere over time in terrestrial ecosystems. In spite of a different sensitivity to climate
86 drivers (Baldocchi, 2008), GPP and Reco are generally strictly related since photosynthetic
87 assimilated carbon constitutes the substrate for autotrophic respiration (Collalti et al., 2020) and
88 also stimulates soil (Davidson et al., 2006) and heterotrophic respiration (Migliavacca et al.,
89 2015, 2011). However, several studies have reported a decoupling of the two processes
90 (Baldocchi and Penuelas, 2019; El-Madany et al., 2020; Ma et al., 2019; Migliavacca et al.,
91 2015; Reichstein et al., 2007), mainly resulting from differences in the response to climate
92 drivers or substrate availability. For example, in an oak-grass savanna in California, a
93 decoupling was observed at the beginning of the autumn season when the presence of litter
94 stimulates the heterotrophic respiration, before the understorey was sufficiently developed to
95 contribute to the overall GPP (Ma 2016).
96 Temperature, precipitation and radiation are well known drivers of the variability of CO_2
97 exchange in different ecosystems (e.g. Fu et al., 2019; Jung et al., 2017; Marcolla et al., 2011;
98 Wang et al., 2014). Likewise, vegetation traits such as biodiversity and ecosystem structure, are
99 known to influence NEE variability (Anderegg et al., 2018; Musavi et al., 2017;
100 RICHARDSON et al., 2007). Additionally, phenology can have a large impact on both
101 photosynthesis and respiration, hence the analysis of phenological patterns may help explain
102 observed trends in GPP and Reco. In cork oak woodlands, only the herbaceous understory

shows marked seasonal patterns while evergreen trees maintain similar canopy cover all year round (Cerasoli et al., 2016) and the impact of understory phenology on carbon fluxes is difficult to ascertain and rarely considered (Correia et al., 2016; Ma et al., 2007).

Water availability is a major environmental factor constraining NEE fluxes in Mediterranean forests, controlling photosynthetic carbon assimilation rate and dampening respiration fluxes during dry hot periods (Pereira et al., 2007). Given the proneness of Mediterranean ecosystems to long dry periods, a better understanding of climate-ecosystem interactions demands a corresponding understanding of the impact of drought on GPP and Reco. Drought events can have a strong influence on the inter-annual variability of NEE as demonstrated in studies considering diverse terrestrial ecosystems and climatic zones (Baldocchi et al., 2018; Zscheischler et al., 2014).

Total annual precipitation contributes to the replenishing of soil moisture and groundwater resources allowing deep-rooted oak trees to survive the dry season (David et al., 2016). As such, understanding the response of Mediterranean ecosystems to rainfall variability at annual scales is essential to anticipate the potential effects of future climate change and increasingly frequent extreme events (Reichstein et al., 2013).

Changes in rainfall timing also have an impact on the growing season length (GSL) of the herbaceous layer. While a delay in autumn rains postpones the start of the season (Luo et al., 2018; Nogueira et al., 2017), in spring rainfall scarcity and high temperatures accelerates the dry-down period (Cerasoli et al., 2018). Hence, in addition to total rainfall, rainfall timing largely influences the carbon fluxes in cork oak woodlands, in particular those that have a considerable contribution from shrubs and grasses to the overall carbon balance (Correia et al., 2016; Dubbert et al., 2014; El-Madany et al., 2018; Luo et al., 2020; Piayda et al., 2014).

Furthermore, under expected conditions of high temperature and low soil moisture, transpiration of trees and grass is constrained and vapor pressure deficit (VPD) increases, further exacerbating water stress (Seneviratne et al., 2010). Hence, together with rainfall, VPD can also influences the length of the growing season of the herbaceous vegetation.

Examining the inter-annual variability of the start and end of the understory growing season is therefore crucial to our understanding of the impact of expected exacerbated water scarcity on the ecosystem carbon balance.

Carbon flux dynamics are not controlled only by their instantaneous dependency on climate and vegetation but also on time lagged effects (Besnard et al., 2019). However, in most of the studies only the direct effect of climate variables is considered, while the time lagged effect is generally ignored (Zhang et al., 2015). Considering the importance of time lagged effects, can contribute for our understanding of long term ecosystem responses to climate disturbances (Marcolla et al., 2011). The analysis of the inter-annual variability of carbon and respiration fluxes should therefore consider altogether climate drivers, vegetation traits and possible legacy effects to improve our understanding of factors controlling carbon exchange. Long-term datasets are necessary to observe processes at different time scales and to reveal short-term dependencies and legacy effects. Notwithstanding, few studies analysing the inter-annual variability of carbon fluxes have focused on Mediterranean oak woodlands (Costa-e-Silva et al., 2015; El-Madany et al., 2020, 2018; Ma et al., 2016).

In this work, we analyse seven years (2010–2017) of continuous eddy covariance (EC) flux measurements at a Mediterranean cork oak woodland to: i) evaluate the impact of rainfall timing and magnitude on carbon fluxes at inter-annual and seasonal scales; ii) identify any potential legacy effects, and quantify the corresponding time lags, between rainfall and carbon fluxes dynamics; and to iii) investigate the sensitivity of ecosystem carbon fluxes to the understory GSL and if such sensitivity is mediated by precipitation and VPD. The hypothesis tested is that the duration of the understorey GSL has a significant impact on the annual fluxes and that it is affected not only by water scarcity close to the emergence and senescence of the understorey but also by winter precipitation.

2. Materials and methods

2.1 Study site

Our study was conducted in a 50-year-old cork oak woodland (*Quercus suber* L.) at Herdade da Machoqueira do Grou, located in Central Portugal (39° 08′ 20.9″ N, 9° 19′ 57.7″ W, 165m altitude). The climate is Mediterranean, with mild, wet winters and hot, dry summers. Long term (1981–2010) mean annual rainfall is 653 mm and mean annual temperature is 16.2 ± 4.7 ºC (IPMA (Instituto Portugûes do mar e da Atmosfera), n.d.). The soil is a cambisol (FAO-UNESCO, 1974), with 81% sand, 5% clay and 14% silt. Tree density is 177 tree ha^{-1} and tree leaf area index (LAI) is 1.6 m^2 m^{-2} (Correia et al., 2014). At the beginning of the measurement period the mean height below the canopy and total height of trees was 3.1 and 7.9 m, respectively and the mean diameter at breast height was 24.7 cm (Costa-e-Silva et al., 2015). Cork oak canopy cover at the site is 36% and the understory layer is composed by a mixture of shrubs and herbaceous species. The site was ploughed in 2009 (Correia et al., 2016) and 2013, hence the shrubs cover fraction changed across years. A field survey in 2017 measured a 18% coverage of shrubs and 41% of herbaceous species, with litter and bare soil covering the remaining area (Heuschmidt et al., 2020). *Cistus salviifolius* and *Ulex airensis* are the most represented shrubs species, while grasses (44.5%) and legumes (28.7%) dominate the herbaceous layer (Xavier Lecomte, personal communication).

2.2 Climatic drivers and ecosystem carbon fluxes

Carbon dioxide (CO_2) and water vapor fluxes were measured continuously by eddy covariance from September 2010 to August 2017. The equipment is positioned at the top of a 22 m tower and consists of a 3D sonic anemometer (R3, Gill Instruments Ltd., Lymington, England) and a closed-path infrared gas analyser (IRGA, Li 7000, Li-Cor Inc., Lincoln, NE, USA). Precipitation (ARG100, Environmental Measurements Ltd., Gateshead, UK), solar radiation (BF2, Delta-T Devices Ltd., Cambridge, UK), humidity and air temperature (CS215, Campbell Scientific, Inc., Logan, UT, US) were collected by a data logger (CR1000, Campbell Scientific, Inc., Logan, UT, USA) and averaged at a 30-minutes time step (Costa-e-Silva et al., 2015).

Flux data were processed with the EddyPro software (version 6.2.0, LI-COR Biosciences Inc., Lincoln, NE, USA). Raw data were first despiked according to Vickers and Mart (1997). Time lags were then determined by a procedure accounting for the dependency of water vapor lags to relative humidity. Coordinates rotation followed the planar fit method (Wilczak et al., 2001) for the main wind directions between 15º-90º and 200º-330º, while the double rotation was applied for wind directions comprised between 90º-200º and between 330º-15º. With this approach we tested the influence of the potential flux contribution of a rain-water-harvesting lake and an eucalypt area in the 80% iso-line of the footprint climatology (Kljun et al., 2015). The estimate of the u* threshold (Papale et al., 2006), gap filling and flux partitioning were performed using the REddyProc R package (Wutzler et al., 2018). The average u* threshold was 0.32 (±0.030). After correction of CO_2 fluxes for storage (using the one-point storage correction), the NEE was partitioned into GPP and Reco according to Reichstein et al. (2005). We follow the convention that negative NEE represents a carbon sink and positive NEE represents a carbon source at the surface, thus, GPP=-NEE + Reco. Further details on eddy covariance data processing and the dataset used are openly available (Cerasoli et al., 2020).

The soil water content (SWS) was calculated at daily time step adopting the one-layer bucket concept (Manabe, 1969). At each day (t),

$SWS(t) = SWS(t-1) + R(t) – E(t);$

Being the recharge $R(t)= \min[P(t), SWS_{max} - SWS(t-1)]$

and the daily evapotranspiration E(t) calculated from latent heat values.

The maximum water content (SWS_{max}) or field capacity was estimated to be 200mm and the permanent wilting point, the lower value of SWS that still permits water extraction by plants, was fixed at 7.5mm with basis on 10cm depth soil measurements done in previous studies carried out at the site (Jongen et al., 2013).

2.3 Extraction of seasonality parameters

Phenological parameters were estimated from remote-sensed time-series data, Here, we used the TIMESAT software package (Jönsson and Eklundh, 2002, 2004) to analyse a time-series of

NDVI (Tucker, 1979) data of the study area derived from quality-controlled MODIS bands. The daily MODIS collection MCD43A4, at 500m spatial resolution (Schaaf and Wang, 2015a), was downloaded from the Google Earth Engine (GEE) platform (Gorelick et al., 2017) (https://earthengine.google.com) for a 2km radius circular area centred around the tower location. The MCD43A2 product (Schaaf and Wang, 2015b) was used to control for the quality of the BRDF inversion for each surface reflectance band and filter out observations with clouds and water coverage. A mean value of the good quality pixels was then obtained for each MODIS band used to calculate NDVI (Supplement material, fig. S1).

The program first fits smooth functions to the data, in this study the Savitzky-Golay filter was selected (Savitzky and Golay, 1964), and once the fitting has been achieved, it computes seasonality parameters such as the start (SOS), the end (EOS) and the length of the growing season length (GSL). An anticipation of the SOS and/or a delay in the EOS result in an increase of GSL. These parameters give important information about short- and long-term vegetation changes, and their dependency on climate, providing insights on the functional and structural characteristics of the ecosystem. Despite the complex multilayer composition of vegetation at the site, we are confident that the temporal NDVI trend realistically represents the phenology of the herbaceous understory.

Indeed, spectral measurements of the different vegetation types, collected *in-situ* and for the same period considered in this study, showed a marked NDVI seasonal trend of the herbaceous layer and very constant values for the evergreen cork aok canopy (Soares et al., 2022).

In addition, a simulation analysis, revealed that even when the tree density is high, the variability of MODIS NDVI is mainly driven by the herbaceous layer (Häusler et al., 2016).

2.4 Data analysis

Meteorology and carbon flux data from 2010 to 2017 were analysed and hereafter reported by hydrological year, considered running from September 1 to August 31 based on the rainfall pattern in the region. For seasonal analyses, we considered the following periods: autumn (September, October, November), winter (December, January, February), spring (March, April,

May) and summer (June, July August). A 30-day moving average was used to visualize temporal patterns of carbon fluxes, daily mean temperature and global radiation.

The occurrence of time lags between rainfall and carbon fluxes (GPP, Reco and NEE) was addressed by computing the correlation between 12 months cumulative values of the variables differing one month from each other. The multiple "yearly" values of carbon fluxes obtained were correlated with those of rainfall considering different potential time lags by using a moving time window ranging from 0 to 12 months and shifted three months at a time (Marcolla et al., 2011).

All statistical analyses were performed using R (R CoreTeam, 2016). One-way ANOVAs were performed to evaluate the significance of variance between seasons and years of GPP, Reco and NEE measurements. Conditions of homoscedasticity and normality were always verified by visual inspection of residuals. To estimate which climate variable controls SOS and EOS of the growing season of the understory vegetation we correlated total precipitation and the average maximum vapor pressure deficit to each phenological date using both linear and quadratic models. Models with the greatest coefficient of determination (adjusted R^2) were selected. The time span considered for correlation with the SOS was September-October since data showed that SOS was always comprised between the end of September and the beginning of October. For EOS both seasonal and bi-monthly time spans were used. Only regression with $p \leq 0.05$ were considered. The inter-annual anomalies of GSL (ΔGSL) have been calculated as the difference between values estimated from a regression line fitted to all years and the observed annual values. Linear regression models were applied to estimate the impact of ΔGSL on carbon fluxes (GPP, Reco and NEE).

3. Results

3.1 Time series of CO_2 fluxes and meteorological variables

In spite of a moderate difference among records of average daily temperature within the analysed period (Tmin = 10.9 ± 4.5 ºC; Tmax = 21.4 ± 7.2ºC; Tmean = 15.7 ± 5.5 ºC for 2010-

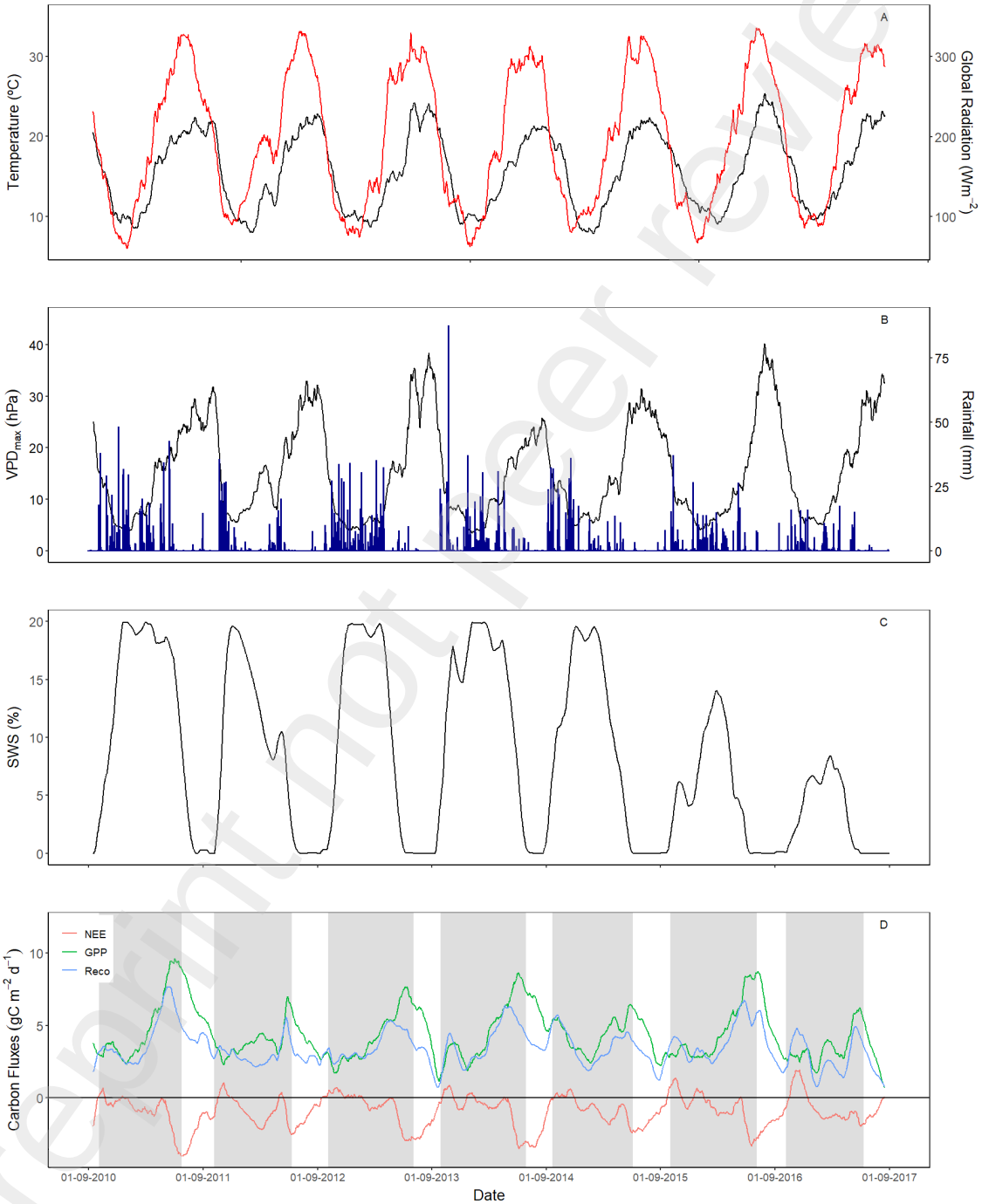

Fig.1 Daily values of average temperature (black line, ºC), average global radiation (red line, W m^{-2}) (A), maximum VPD (black line, hPa) and total Rainfall (blue bars, mm) (B), soil water storage (%) (C) and Carbon Fluxes (g C m^{-2} d^{-1}) (D). With the exception of rainfall all variables are represented as 30-days moving averages. Shaded areas (D) represent the growing seasons length (GSL) of the herbaceous understory. Data shown have been recorded at the site between September 2010 and August 2017.

2017) a marked seasonality was observed (Fig. 1A). The maximum and the minimum daily average temperatures were always recorded in summer and winter, respectively. Daily average temperature and global radiation (Fig. 1A)were highly correlated (R^2=0.71; p-value <0.001). Total rainfall was generally concentrated in autumn and winter (Fig. 1B). On the opposite, the maiximum vapor pressure deficit (VPD_{max}) was higher during the summer period (Fig. 1B), in agreement with the temperature trend observed. The Soil Water Storage (SWS, Fig.1C) followed roughly seasonal rainfall patterns, being higher in winter and decreasing sharply in summer to recover only after the occurrence of first rains in September The extent of the dry summer period (consecutive days with SWS<7.5%) varied among years, ranging from 80 days in 2014 to 149 in 2016. The impact of low winter rainfall on the SWS is particularly evident in the last two years of the study when the SWS never reach its maximum.

Ecosystem carbon fluxes also showed a marked seasonality (Fig 1D), typical of Mediterranean oak woodlands. Each year, a tendency for higher NEE with the onset of spring was observed, while GPP and Reco showed a positive trend. At the end of the herbaceous understory growing season (shaded areas, Fig. 1D), the NEE trend was generally inverted as a result of a drop in GPP and Reco towards summer and beginning of autumn. During these periods, Reco flux rates were occasionally higher than GPP causing NEE to approach zero or to become slightly positive and the ecosystem to temporarily function as a carbon source.

3.2 Inter-annual and seasonal variability

A large inter-annual variability was observed for rainfall (p-value<0.001), with autumn, winter and spring rainfall being highly variable between years (Fig. 2A). Total annual rainfall during the study period was 43%, 18% and 28% higher than the long-term average of 623 mm in 2010–2011 (928 mm), 2012-2013 (765 mm) and 2013-2014 (830 mm), respectively, and 37%, 22%, 21% and 44% lower in 2011–2012 (408 mm), 2014-2015 (580 mm), 2015-2016 (511 mm) and 2016-2017 (360 mm), respectively.

A high inter-annual variability was also observed in carbon fluxes. The average annual NEE was -338 ± 70 g C $m^{-2}y^{-1}$, ranging from -460 $gCm^{-2}y^{-1}$ to -251 $gCm^{-2}y^{-1}$ (Fig. 2B). There were significant differences among years (p-value<0.001), but the ecosystem acted as a carbon sink (i.e. annual NEE<0) in all the seven years of the study.

The annual GPP was on average 1598 ± 227 $gCm^{-2}y^{-1}$ ranging from 1187 $gCm^{-2}y^{-1}$ to 1905 $gCm^{-2}y^{-1}$, while average annual Reco was 1260 ± 181 $gCm^{-2}y^{-1}$, ranging from 936 $gCm^{-2}y^{-1}$ to 1445 $gCm^{-2}y^{-1}$. The maximum and minimum values of NEE, GPP and Reco were observed in 2010/2011 and 2016/2017, respectively. Annual GPP showed significant inter-annual variability (p-value<0.001), with some years being more productive (2010/11, 2013/14 and 2015/16) than the average and a clear tendency of summer and spring to be the most productive seasons of the year (Fig. 2C).

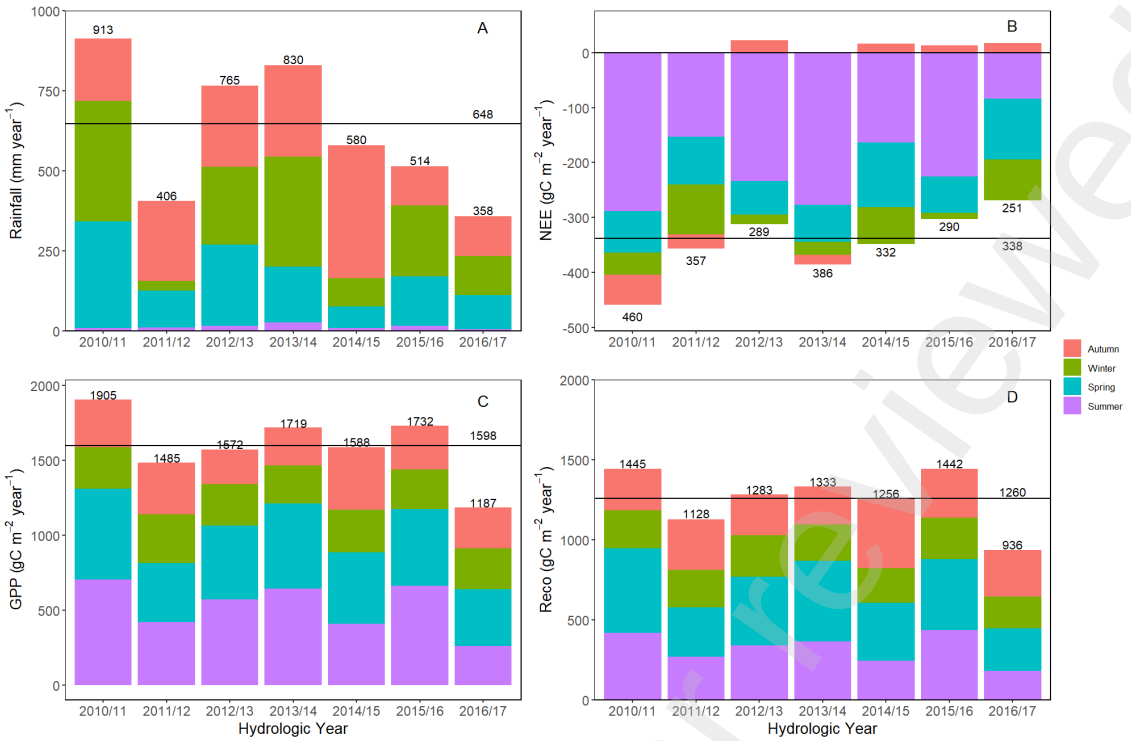

Fig.2 Cumulative values of Rainfall (A, mm year^{-1}), NEE (B, gC m^{-2} year^{-1}), GPP, (C, gC m^{-2} year^{-1}) and Reco (D, gC m^{-2} year^{-1}) All variables are grouped by hydrological year and partitioned into seasons. Black line represents the average over the study period.

At the annual scale, Reco showed patterns similar to those observed for GPP (Fig. 2D) and the two fluxes were strictly correlated (r=0.97). However, the degree of correlation between daily sums of GPP and Reco were different among seasons. A tight GPP-Reco relationship was observed in summer (r=0.89) and spring (r=0.76), while it was weaker in autumn (r= 0.49) and winter (r=0.40), suggesting a potential GPP-Reco decoupling in these seasons. We are aware that the GPP and Reco relationship might be partly spurious because it is derived from the flux partitioning methods. Therefore, we used night-time NEE in place of Reco and midday NEE in place of GPP as an alternative proxy to test for the relationship between the two biological processes. The obtained results showed a less tight but consistent correlation than the ones reported between GPP and Reco fluxes (r=0.69, 0.31, 0.19 and 0.005 for summer, spring, autumn and winter respectively), giving us confidence that the relationship between

photosynthesis and ecosystem respiration found is not impacted by the potential spurious correlation between GPP and Reco.

Spring and summer contributed more to the annual NEE, while autumn showed the largest variability, with the ecosystem acting as a carbon source in autumn of 2012/2013, 2014/2015, 2015/2016 and 2016/2017.

3.2 Rainfall and carbon fluxes

The sign, magnitude and delay of the response of carbon fluxes to rainfall were investigated by the analysis of time-lagged correlations between NEE, GPP, Reco and rainfall (Fig. 3).

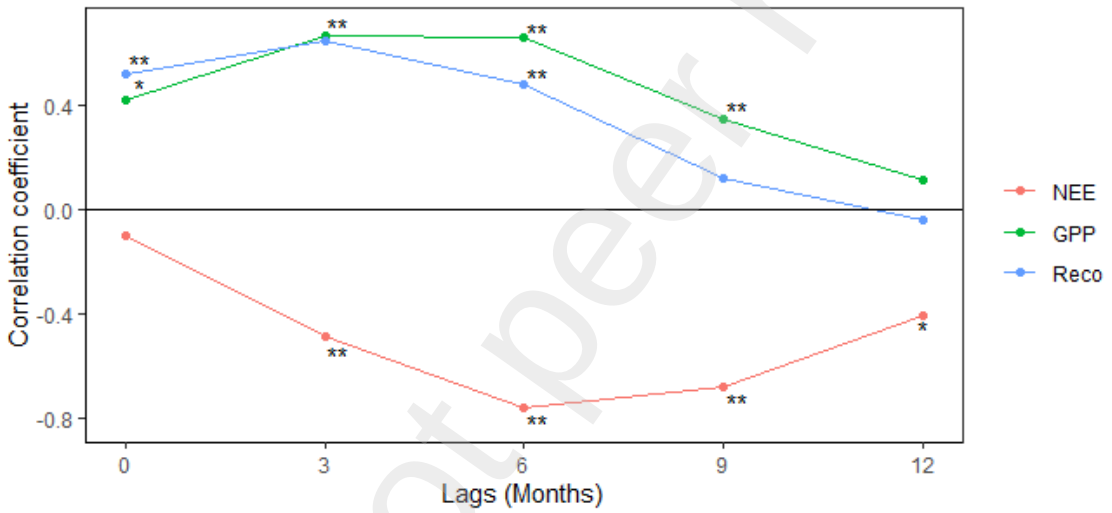

Fig.3 Correlation coefficients observed between annual carbon fluxes and annual rainfall repeated at different time lags in which rainfall precedes carbon fluxes of 0 to 12 months *Correlations significant at the 95 %; **correlations significant at 99 %.

At 0 and 3 months' time-lag, GPP and Reco correlations with rainfall were significant and of similar magnitudes. At longer time lags, the Reco-rainfall correlation was weaker than that observed for GPP-rainfall but still significant at 6 months' time-lag. For GPP the degree of correlation decreased only after 6 months' time-lag onward and was still significant at a 9 months' time-lag. As a result differences were observed between GPP-Rainfall and Reco-Rainfall correlations. The association between NEE and Rainfall was not significant at 0 time-

lag but increased progressively at 3 and 6 months' time lag, when reached a peak and then decreased at 9 and 12 months' time-lag but maintaining a significant degree of correlation.

3.4 Growing Season length

Growing season start (SOS), end (EOS), and length (GSL) obtained by the analysis of NDVI time series are represented as grey shades in Figure 1B and summarized in Table 1. We observed high inter-annual variability in all the parameters, with differences in the SOS of about 16 days varying from the day of the year (DOY) 263 in 2014/2015 to the DOY 279 in 2011/2012 and 2016/2017. In 2014/2015 the earlier SOS coincided with an anomalous high precipitation recorded in September 2014. The variability of the EOS was 31 days, larger than that of the SOS ranging from DOY 154 in 2014/2015 to DOY 185 in 2015/2016. Similarly, GSL showed an inter-annual variability of 29 days ranging from 247 days (2011/2012 and 2016/2017) to 276 days (2015/2016).

Table 1 Seasonality parameters extracted from TIMESAT analysis of NDVI time series: start of the growing season (SOS, doy), end of the growing season (EOS, doy) and the growing season length (GSL, nº of days).

Hydrologic year	**GSL (nº of days)**	**SOS (doy)**	**EOS (doy)**
2010/2011	264	276	175
2011/2012	247	279	162
2012/2013	271	278	184
2013/2014	274	270	179
2014/2015	256	263	154
2015/2016	276	274	185
2016/2017	247	279	161

The dependency of SOS and EOS on rainfall and vapor pressure deficit (VPD_{max}) was tested by regression analyses for different time periods preceding the occurrence of the event. Over the

study period, the SOS was clearly influenced by rainfall at the beginning of the hydrologic year (September-October) (figure 4, A). being delayed when it was scarce and anticipated under opposite conditions. On the contrary, the daily average of the maximum vapor pressure deficit over the same period (VPDmax) showed negative trend with SOS, resulting in a delay of the SOS as VPD increases (figure4, B).

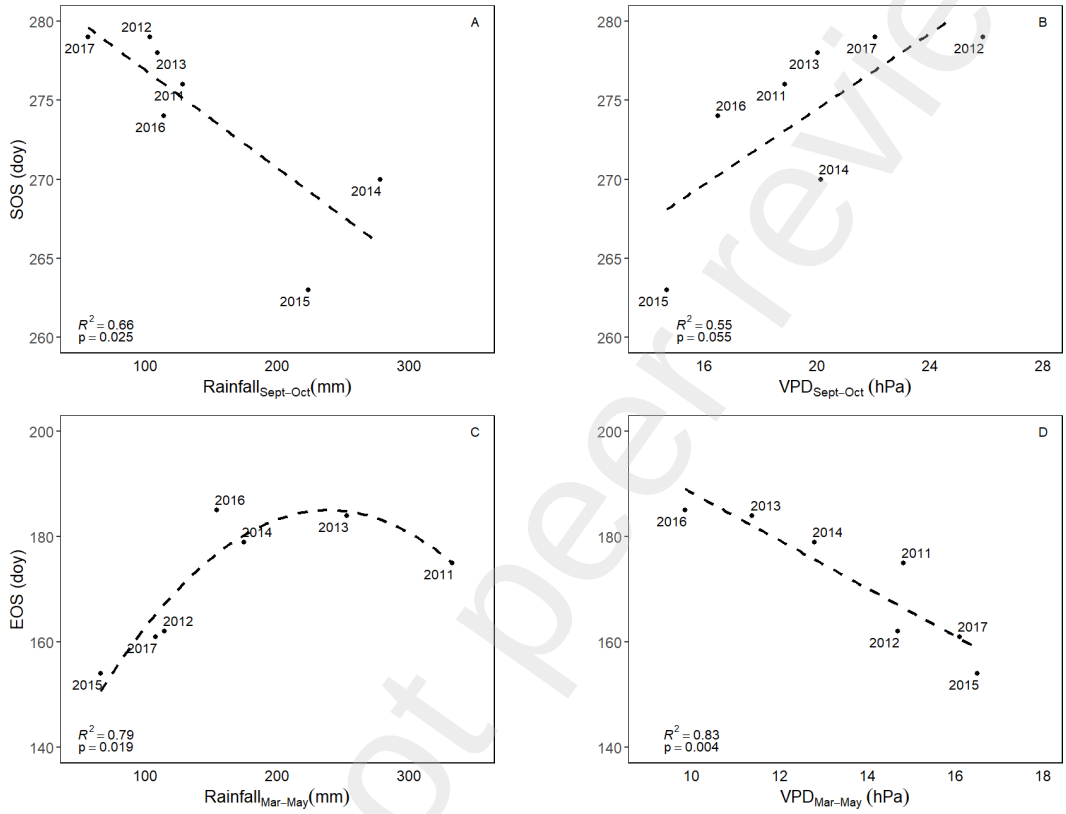

Fig. 4 Relationships between the Start of the season (SOS) and September –October total rainfall (A), and vapor pressure deficit (B); relationship between the End of the Season (EOS) and March-May total rainfall (C) and vapor pressure deficit (D).

Opposite trends to the observed for the SOS were observed assessing the sensitivity of EOS to climate variables. The EOS was found significantly sensitive to Rainfall and VPD in Spring (March-May) (Fig.4, C and D) just before the onset of senescence. The quadratic regression observed indicates that the dependency of EOS on rainfall, is particularly strong for rainfall values up to about 230 mm when the fitted curve reached its maximum while at higher rainfall values the sensitivity seems to decrease (Fig. 4, C). Instead, the sensitivity of the EOS to VPD

in spring was linear, showing a sharp anticipation in the EOS as VPD increases. EOS was particularly anticipated in 2015 which exhibited the lower rainfall and higher VPD in Spring. Noticeably a significant regression was also verified between EOS and total Rainfall recorded in January and February (y=0.125R+155, R^2=0.642, p=0.03). Any other time period did not result in any significant correlation.

Table 3. Regressions between GPP, Reco and NEE and the inter-annual variability of the growing season length (ΔGSL). Fluxes are accumulated values by hydrologic year (year) and by summer.

	year	summer
GPP	12.3ΔGSL+1598; R^2=0.44, p=0.10	11.04ΔGSL+526; R^2=0.69, p=0.021
Reco	11.7ΔGSL+1260; R^2=0.63, p=0.033	6.34ΔGSL+322; R^2=0.68, p=0.022
NEE	-0.62ΔGSL-338; R^2=0.01, p=0.818	-4.70ΔGSL-204; R^2=0.66, p=0.036

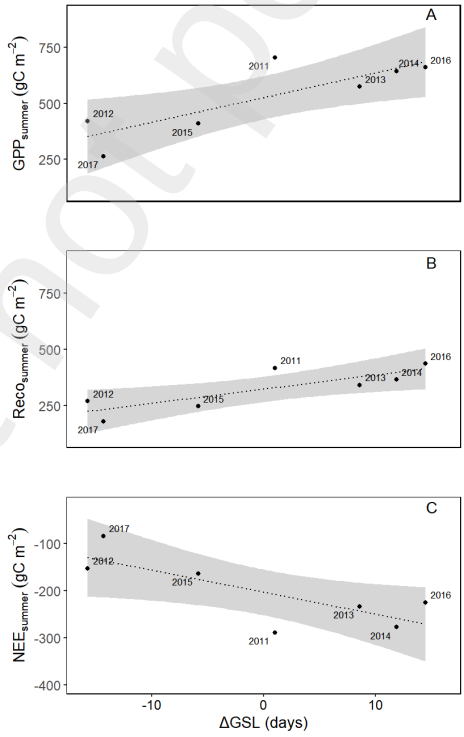

Fig. 5 Relationship observed between GPP (a), Reco (b) and NEE (c) (gCm-2) accumulated during the summer period and the anomalies of the growing season length (ΔGSL). The labels

refer to the year. Equations are reported in table 3. The shaded areas represent the 95% confidence interval.

Differences in the SOS and EOS resulted in inter-annual differences of the GSL. We verified the impact of the inter-annual anomalies of the growing season length (ΔGSL) on carbon fluxes at annual and seasonal time scale. Carbon fluxes accumulated during the summer period were significantly impacted by ΔGSL . Each additional day of the GSL resulted in an additional uptake of 11gC m^{-2} (Table 3, Fig.5A,), an extra respiratory loss of 6.3 gC m^{-2} (Table 3,Fig.5B) and thus an additional net carbon sequestration of 4.70 gC m^{-2} (Table 3, Fig.5C).

At annual scale, the impact of the ΔGSL on GPP and Reco was similar, but Reco was almost twice than the observed in summer, indicating differences in the GPP/NEE ratio along the year. As a consequence of the GPP-Reco decoupling, GSL has no influence on the annual NEE.

4. Discussion

4.1 Inter-annual and seasonal variability

The study site showed a considerable ability to act as carbon sink. The observed average annual NEE (-338 $gCm^{-2}y^{-1}$) was in agreement with what was previously observed at the same site (Costa-e-Silva et al., 2015) but higher than values recorded at other similar ecosystems. For example, in a mixed cork (*Quercus suber* L.) and holm oak (*Quercus ilex* spp. rotundifolia) in a southern Portuguese site, NEE ranged between -140 and -28 $gCm^{-2}y^{-1}$ (Pereira et al., 2007). In two other holm-oak woodland sites in the nearby region of Extremadura (Spain) the average annual NEE recorded was 75 and 15 $gCm^{-2}y^{-1}$ (El Madany, 2020) and in a Californian site, NEE was about -110 $gCm^{-2}y^{-1}$ (Ma et al., 2016).

Differences in climate and vegetation among sites make it difficult to discern reasons for the higher carbon sequestration observed in this study as compared to other Mediterranean oak woodlands. A possible distinguishing feature could be the higher evergreen tree canopy cover

(around 40% in this study, against 19-24% in the other mentioned studies) and consequently a higher contribution of tree photosynthesis to the overall GPP. Cork oak trees are drought avoiding species, relying on deep roots and a tight stomatal control to escape summer drought conditions (David et al., 2016). This efficient strategy allows trees to recover rapidly transpiration and carbon assimilation rates when drought conditions are alleviated (Caldeira et al., 2015). Hence, a higher tree density can contribute to maintain a positive carbon sequestration (negative NEE), as compared to sites where the understory, dependent on shallow soil water, represents a larger fraction of the overall GPP. The presence of semi-deciduous and evergreen shrubs in the understory could also have contributed to maintain GPP during summer dry periods (Correia et al., 2014). However, shrubs were regularly removed (every 3-4 years) and their contribution varied across time.

Despite the consistent annual carbon sequestration, we observed significant inter-annual and seasonal differences in NEE, GPP and Reco. Spring and summer carbon assimilation contributed most to the annual GPP, similar to what was observed in a Californian savanna-type ecosystem (Ma et al., 2016). Summer was also the season in which we observed the largest inter-annual variability in NEE and a tight GPP-Reco coupling, suggesting that Reco was strictly dependent on GPP during that season and that the observed variability in summer NEE was related mainly to constraints in photosynthetic carbon assimilation.

In four of the seven years analysed, NEE became positive in autumn and the ecosystem switched then to a carbon source. A positive NEE was observed in years with below average summer rainfall (2012/2013, 2015/2016 and 2016/2017), suggesting that the critical depletion of soil moisture was responsible for the observed decrease of GPP and in a lesser extent of Reco at the beginning of the hydrological year.

A positive NEE in the autumn season was also observed under opposite conditions, amore than average rainy summer and autumn (2014/2015). In this year, both GPP and Reco were above the long-term average but the proportion was slightly higher for Reco than GPP (see section 3.2). The increased proportion of Reco could be partly ascribed to a high heterotrophic respiration at the beginning of the autumn season (El-Madany, 2020). A similar pattern was also

observed under low water availability conditions, particularly under isolated rain pulses (Fraser et al., 2016; Jarvis et al., 2007).

A low degree of correlation between GPP and Reco was also observed in winter. In winter months, when usually soil water is not a limiting factor, GPP can be constrained by low radiation and temperature. On the opposite, Reco is driven mainly by temperature and hence a decoupling between GPP and Reco can occur.

4.2 The long-term impact of Rainfall

The importance of rainfall for ecosystem survival in semi-arid ecosystems is unquestionable and several studies have highlighted that carbon fluxes in Mediterranean ecosystems are strongly affected by the erratic seasonal and inter-annual distribution of rainfall events (Almagro et al., 2009; Jongen et al., 2011; Pereira et al., 2007; Poulter et al., 2014; Reichstein et al., 2002; Ross et al., 2012). Our results show that rainfall has a time-lagged impact on NEE that extend up to a 12 months delay. As observed in other studies (Marcolla et al., 2011), the time-lagged effect was stronger than the concurrent effect. The strongest correlation between rainfall and carbon fluxes was observed at 3 and 6 -month time lags. The reason behind this long time-lagged effect can be partly explained by the existence of a water table reservoir accessible by deep oak roots that likely promotes inter-seasonal rainfall mixture (Costa-e-Silva et al., 2015). In addition to the ability to extract water from deep soil layers (Costa-e-Silva et al., 2015; Pinto et al., 2014), cork oak trees can also redistribute it to the soil surface through the hydraulic lift (Pinto et al., 2014). This process alleviates summer stress conditions and can decrease the ecosystem dependency on recent rainfall (David et al., 2016). Indeed, in woodlands with a lower tree cover fraction, GPP was found largely dependent on short term rainfall (Luo et al., 2020, 2018). An analysis of past conditions' influence on ecosystem carbon exchange across different ecosystem types, revealed that about 32% of the variation in NEE was explained by previous conditions and that environmental memory was primarily driven by soil moisture (Liu et al., 2019). Such time-lagged effects could enhance the ecosystem's resistance to more frequent climate extremes and deserves a better consideration in the evaluation of ecosystem stability. A deeper knowledge

of lag effects could advance our understanding of the mechanisms responsible for climate change effects on ecosystem carbon fluxes.

We observed an almost parallel trend in GPP and Reco correlation with rainfall as the time lag increased (Fig.4). However, while at short time lags (0 and 3 months) the correlation coefficients were very similar for the two fluxes, beyond a 6-month lag the correlation was consistently higher for GPP. The presence of the water table may also explain this observation by acting as a long-term reservoir of rainfall and allowing higher GPP rates while Reco, which is partly dependent on heterotrophic respiration, would be more strongly related with short term rainfall (0 and 3 months). These different dependencies are in agreement with the observed GPP-Reco decoupling.

4.3 The Relationship between rainfall, growing season length and carbon fluxes

In this study, remotely-sensed data were used to retrieve the start (SOS), the end (EOS) and the length (GSL) of the growing season of the understory vegetation. Even though multi-layer vegetation strata are present at the site, we are confident that the extracted seasonality parameters represent changes in the annual growing seasonal cycle of the herbaceous vegetation and semi-deciduous shrubs. In fact, previous analyses of in-situ spectral retrievals data collected at the same site, showed a fairly constant NDVI trend of cork oak canopy across seasons and years but a large NDVI inter-annual variability for the herbaceous layer, in agreement with the variability of the phenological parameters observed in the present study (Cerasoli et al., 2016; Soares et al., 2022). The GSL observed at our site was also in line with an average GSL of 200-300 days for savanna ecosystems reported in a global synthesis from Baldocchi et al. (2008).

Both rainfall and VPD recorded in the months previous to the phenological events showed clearly to influence both the start (SOS) and the end of the season (EOS). The dependency of the SOS on rainfall observed at the beginning of the hydrological year (September- October) was already reported in other studies in similar ecosystems and climate conditions (Luo et al., 2020; Nogueira et al., 2017). Equally, the dependency of the EOS on spring rainfall and VPD was reported in previous studies (Marchin et al., 2018).

In our study, a larger variability of the end of the season (EOS) than the start of the season (SOS) dates was observed, emphasizing the high sensitivity of the understory to summer drought conditions. Ma and colleagues (2007) reported that the lack of precipitation in the spring (April, May and June) was one of the predominant factors affecting the length of the growing season in a oak-grass savanna in California.

Similarly to what reported in other studies (Marchin et al., 2018), our results also evidence the role of VPD to predict the timing of grass green-up (SOS) and yellowing (EOS). The VPD is a measure of the atmosphere humidity which is known to be related to evapotranspiration and hence also to the physiological response of vegetation to soil water deficit. Here, the strong and linear correlation observed between EOS and VPD evidence the sensitivity of the herbaceous layer to atmospheric humidity and temperature and their influence on the timing of phenological events.

In agreement with previous studies at the same site (Correia et al., 2016; Piayda et al., 2014)., the EOS was also found dependent on winter rainfall suggesting a delay in the impact of precipitation also for the growing season length of the herbaceous understory

The relevance of winter rainfall is probably a consequence of the annual rainfall distribution, mainly concentrated in winter, and hence contributing most to the overall annual rainfall. On the contrary, summer precipitation represents only 1-3% of the total annual rainfall. Hence, the strong EOS-rainfall correlation observed in this period highlights the importance of precipitation timing for the onset of senescence of the understory vegetation.

The tested hypothesis that the duration of the GSL could significantly impact annual carbon fluxes was only partially confirmed. The increase of the GSL observed at our site leads to positive anomalies of the annual gross fluxes (GPP and Reco) but not of NEE. In fact, the relationship NEE-ΔGSL at the annual scale was not significant neither strong (0.6 gC m^{-2}, Table 3). This is in contrast with previous studies that showed a significant relationship between GSL and NEE for savanna and forest ecosystems (Baldocchi, 2008; Richardson et al., 2010).

However, the impact of ΔGSL was significant on summer fluxes. These results confirm the importance of precipitation timing, indicating that a small amount of precipitation can delay the onset of senescence resulting in a considerable gain in ecosystem GPP and NEE.

5. Conclusions

In this study we evaluate the long-term impact of rainfall on a cork oak woodland carbon fluxes. This knowledge can contribute to foresee the ecosystem's response to climate change conditions and support forest management actions in order to maximize productivity and ecosystem services. We argue that the long time lag between rainfall and carbon dynamics was determined mainly by the high tree density, which may confer long-term stability to the ecosystem. However, progressive drought conditions reported in recent years have been responsible for an increase in tree mortality and decline (Camilo-Alves et al., 2017) and further studies should focus on the ability of trees to overcome expected exacerbated droughts.

Our results also highlight the sensitivity of the understory to the rainfall regime and its associated impact on GPP and Reco. Other studies, employing stable isotopes, demonstrated that the understory can contribute considerably (50%) to the whole GPP and, in spite of a high sensitivity to water shortage, can have a beneficial effect on the resilience of the ecosystem to drought, favouring, for example, soil water infiltration (Dubbert et al., 2014). This shows the importance of considering the interactions between over- and understory to maximize oak woodlands productivity and carbon sequestration.

Overall, our results emphasize the need for a better understanding of the sensitivity of trees and understory vegetation to changes in rainfall regime and underline the importance of considering legacy effects on carbon fluxes. The multi-temporal scale approach appears essential in understanding climate drivers and improving our ability to foresee the impacts of forthcoming climate change on ecosystem carbon exchange.

Acknowledgments

This study was funded by FCT – Fundação para a Ciência e Tecnologia through the project MEDSPEC, Monitoring Gross Primary Productivity in cork oak woodlands through remote sensing and biophysical modelling (PTDC/AAG-MAA/3699/2014) and the research activities of the Forest Research Centre (UIDB/00239/2020). Sofia Cerasoli was funded by PORBIOTA (Portuguese E-Infrastructure for Information and Research on Biodiversity (POCI-01-0145-FEDER-022127), supported by Operational Thematic Program for Competitiveness and Internationalization (POCI), under the PORTUGAL 2020 Partnership Agreement, through the European Regional Development Fund (FEDER). Catarina Moura was supported by a post-doctoral fellowship granted by the MEDSPEC project (PTDC/AAG-MAA/3699/2014).

Authors are grateful to Dr. Simon Besnard for providing the corrected NDVI time series for the site used in this study and to Herdade da Machoqueira do Grou for the permission to undertake research at the study site.

Declaration of Competing Interest

The authors declare that they have no known competing financial interests or personal relationships that could have appeared to influence the work reported in this paper.

Database

Publicly available at https://zenodo.org/record/3727798#.Xqh9dJnOXIV

589 **References**

590

591 Ahlström, A., Raupach, M.R., Schurgers, G., Smith, B., Arneth, A., Jung, M., Reichstein, M.,
592 Canadell, J.G., Friedlingstein, P., Jain, A.K., Kato, E., Poulter, B., Sitch, S., Stocker, B.D.,
593 Viovy, N., Wang, Y.P., Wiltshire, A., Zaehle, S., Zeng, N., 2015. The dominant role of
594 semi-arid ecosystems in the trend and variability of the land CO_2 sink. Science 348, 895–9.
595 https://doi.org/10.1126/science.aaa1668
596 Almagro, M., López, J., Querejeta, J.I., Martínez-Mena, M., 2009. Temperature dependence of
597 soil CO2 efflux is strongly modulated by seasonal patterns of moisture availability in a
598 Mediterranean ecosystem. Soil Biol. Biochem. 41, 594–605.
599 https://doi.org/10.1016/j.soilbio.2008.12.021
600 Anderegg, W.R.L., Konings, A.G., Trugman, A.T., Yu, K., Bowling, D.R., Gabbitas, R., Karp,
601 D.S., Pacala, S., Sperry, J.S., Sulman, B.N., Zenes, N., 2018. Hydraulic diversity of forests
602 regulates ecosystem resilience during drought. Nature 561, 538–541.
603 https://doi.org/10.1038/s41586-018-0539-7
604 Baldocchi, D., 2008. TURNER REVIEW No. 15. "Breathing" of the terrestrial biosphere:
605 Lessons learned from a global network of carbon dioxide flux measurement systems. Aust.
606 J. Bot. 56, 1–26. https://doi.org/10.1071/BT07151
607 Baldocchi, D., Chu, H., Reichstein, M., 2018. Inter-annual variability of net and gross
608 ecosystem carbon fluxes: A review. Agric. For. Meteorol. 249, 520–533.
609 https://doi.org/10.1016/J.AGRFORMET.2017.05.015
610 Baldocchi, D., Penuelas, J., 2019. The physics and ecology of mining carbon dioxide from the
611 atmosphere by ecosystems. Glob. Chang. Biol. 25, 1191–1197.
612 https://doi.org/10.1111/gcb.14559
613 Baldocchi, D.D., 2020. How eddy covariance flux measurements have contributed to our
614 understanding of Global Change Biology, Global Change Biology.
615 https://doi.org/10.1111/gcb.14807
616 Besnard, S., Carvalhais, N., Altaf Arain, M., Black, A., Brede, B., Buchmann, N., Chen, J.,

Clevers, J.G.P.W., Dutrieux, L.P., Gans, F., Herold, M., Jung, M., Kosugi, Y., Knohl, A., Law, B.E., Paul-Limoges, E., Lohila, A., Merbold, L., Roupsard, O., Valentini, R., Wolf, S., Zhang, X., Reichstein, M., 2019. Memory effects of climate and vegetation affecting net ecosystem CO2 fluxes in global forests. PLoS One 14. https://doi.org/10.1371/journal.pone.0211510

Bugalho, M.N., Caldeira, M.C., Pereira, J.S., Aronson, J., Pausas, J.G., 2011. Mediterranean cork oak savannas require human use to sustain biodiversity and ecosystem services. Front. Ecol. Environ. 9, 278–286. https://doi.org/10.1890/100084

Caldeira, M.C., Lecomte, X., David, T.S., Pinto, J.G., Bugalho, M.N., Werner, C., 2015. Synergy of extreme drought and shrub invasion reduce ecosystem functioning and resilience in water-limited climates. Sci. Rep. 5, 1–9. https://doi.org/10.1038/srep15110

Camilo-Alves, C.S.P., Vaz, M., Da Clara, M.I.E., Ribeiro, N.M.D.A., 2017. Chronic cork oak decline and water status: new insights. New For. 48, 753–772. https://doi.org/10.1007/s11056-017-9595-3

Cerasoli, S., Campagnolo, M., Faria, J., Nogueira, C., Caldeira, M. da C., 2018. On estimating the gross primary productivity of Mediterranean grasslands under different fertilization regimes using vegetation indices and hyperspectral reflectance. Biogeosciences 15, 5455–5471. https://doi.org/10.5194/bg-15-5455-2018

Cerasoli, S., Costa e Silva, F., Portugal, J., Moura, C.F., Carvalhais, N., Pereira, João S., …, El-Madany, T., 2020. Carbon and water fluxes in a cork oak woodland in Central Portugal [Data set].

Cerasoli, S., Costa e Silva, F., Silva, J.N., 2016. Temporal dynamics of spectral bioindicators evidence biological and ecological differences among functional types in a cork oak open woodland. Int. J. Biometeorol. 1–13. https://doi.org/10.1007/s00484-015-1075-x

Collalti, A., Tjoelker, M.G., Hoch, G., Mäkelä, A., Guidolotti, G., Heskel, M., Petit, G., Ryan, M.G., Battipaglia, G., Matteucci, G., Prentice, I.C., 2020. Plant respiration: Controlled by photosynthesis or biomass? Glob. Chang. Biol. 26, 1739–1753. https://doi.org/10.1111/gcb.14857

645 Correia, A.C., Costa-e-Silva, F., Dubbert, M., Piayda, A., Pereira, J.S., 2016. Severe dry winter
646 affects plant phenology and carbon balance of a cork oak woodland understorey. Acta
647 Oecologica 76, 1–12. https://doi.org/10.1016/j.actao.2016.07.004
648 Correia, A.C., Costa e Silva, F., Correia, A.V., Hussain, M.Z., Rodrigues, A.D., David, J.S.,
649 Pereira, J.S., 2014. Carbon sink strength of a Mediterranean cork oak understorey: how do
650 semi-deciduous and evergreen shrubs face summer drought? J. Veg. Sci. 25, 411–426.
651 https://doi.org/10.1111/jvs.12102
652 Costa-e-Silva, F., Correia, A.C., Piayda, A., Dubbert, M., Rebmann, C., Cuntz, M., Werner, C.,
653 David, J.S., Pereira, J.S., 2015. Effects of an extremely dry winter on net ecosystem
654 carbon exchange and tree phenology at a cork oak woodland. Agric. For. Meteorol. 204,
655 48–57. https://doi.org/10.1016/j.agrformet.2015.01.017
656 David, T.S., Pinto, C.A., Nadezhdina, N., David, J.S., 2016. Water and forests in the
657 Mediterranean hot climate zone: a review based on a hydraulic interpretation of tree
658 functioning. For. Syst. 25, eR02. https://doi.org/10.5424/fs/2016252-08899
659 Davidson, E.A., Janssens, I.A., Lou, Y., 2006. On the variability of respiration in terrestrial
660 ecosystems: Moving beyond Q10. Glob. Chang. Biol. 12, 154–164.
661 https://doi.org/10.1111/j.1365-2486.2005.01065.x
662 Dubbert, M., Piayda, A., Cuntz, M., Correia, A.C., Costa e Silva, F., Pereira, J.S., Werner, C.,
663 2014. Stable oxygen isotope and flux partitioning demonstrates understory of an oak
664 savanna contributes up to half of ecosystem carbon and water exchange. Front. Plant Sci.
665 5, 1–16. https://doi.org/10.3389/fpls.2014.00530
666 Dubrovský, M., Hayes, M., Duce, P., Trnka, M., Svoboda, M., Zara, P., 2014. Multi-GCM
667 projections of future drought and climate variability indicators for the Mediterranean
668 region. Reg. Environ. Chang. 14, 1907–1919. https://doi.org/10.1007/s10113-013-0562-z
669 El-Madany, T.S., Carrara, A., Martín, M.P., Moreno, G., Kolle, O., Pacheco-Labrador, J.,
670 Weber, U., Wutzler, T., Reichstein, M., Migliavacca, M., 2020. Drought and heatwave
671 impacts on semi-arid ecosystems' carbon fluxes along a precipitation gradient. Philos.
672 Trans. R. Soc. B Biol. Sci. 375, 20190519. https://doi.org/10.1098/rstb.2019.0519

673 El-Madany, T.S., Reichstein, M., Perez-Priego, O., Carrara, A., Moreno, G., Pilar Martín, M.,
674 Pacheco-Labrador, J., Wohlfahrt, G., Nieto, H., Weber, U., Kolle, O., Luo, Y.-P.,
675 Carvalhais, N., Migliavacca, M., 2018. Drivers of spatio-temporal variability of carbon
676 dioxide and energy fluxes in a Mediterranean savanna ecosystem. Agric. For. Meteorol.
677 262, 258–278. https://doi.org/10.1016/J.AGRFORMET.2018.07.010
678 FAO-UNESCO, 1974. Soil Map of the World - Volume V. Paris.
679 Faria, T., García-Plazaola, J.I., Abadía, a., Cerasoli, S., Pereira, J.S., Chaves, M.M., 1996.
680 Diurnal changes in photoprotective mechanisms in leaves of cork oak (Quercus suber)
681 during summer. Tree Physiol. 16, 115–123.
682 Fraser, F.C., Corstanje, R., Deeks, L.K., Harris, J.A., Pawlett, M., Todman, L.C., Whitmore,
683 A.P., Ritz, K., 2016. On the origin of carbon dioxide released from rewetted soils. Soil
684 Biol. Biochem. 101, 1–5. https://doi.org/10.1016/j.soilbio.2016.06.032
685 Fu, Z., Stoy, P.C., Poulter, B., Gerken, T., Zhang, Z., Wakbulcho, G., Niu, S., 2019. Maximum
686 carbon uptake rate dominates the interannual variability of global net ecosystem exchange.
687 Glob. Chang. Biol. gcb.14731. https://doi.org/10.1111/gcb.14731
688 Giorgi, F., Lionello, P., 2008. Climate change projections for the Mediterranean region. Glob.
689 Planet. Change 63, 90–104. https://doi.org/https://doi.org/10.1016/j.gloplacha.2007.09.005
690 Gorelick, N., Hancher, M., Dixon, M., Ilyushchenko, S., Thau, D., Moore, R., 2017. Google
691 Earth Engine: Planetary-scale geospatial analysis for everyone. Remote Sens. Environ.
692 202, 18–27. https://doi.org/10.1016/J.RSE.2017.06.031
693 Häusler, M., Silva, J.M.N., Cerasoli, S., López-Saldaña, G., Pereira, J.M.C., 2016. Modelling
694 spectral reflectance of open cork oak woodland: a simulation analysis of the effects of
695 vegetation structure and background. Int. J. Remote Sens. 37, 492–515.
696 https://doi.org/10.1080/01431161.2015.1134847
697 Heuschmidt, F., Gómez-Candón, D., Soares, C., Cerasoli, S., Silva, J.M.N.N., 2020. Cork oak
698 woodland land-cover types classification: a comparison between UAV sensed imagery and
699 field survey. Int. J. Remote Sens. 41, 7649–7659.
700 https://doi.org/10.1080/2150704X.2020.1767822

ICNF, 2019. 6º Inventário Florestal Nacional.

IPCC, 2021. IPCC, 2021: Summary for policymakers, in: Masson-Delmotte, V., Zhai, P., Pirani, A., Connors, S.L., Péan, C., Berger, S., Caud, N., Chen, Y., Goldfarb, L., Gomis, M.I., M., H., Leitzell, K., Lonnoy, E., Matthews, J.B.R., Maycock, T.K., Waterfield, T., Yelekçi, O., Yu, R., B., Z. (Eds.), Climate Change 2021: The Physical Science Basis. Contribution of Working Group I to the Sixth Assessment Report of the Intergovernmental Panel on Climate Change. Cambridge University Press. In press.

IPMA (Instituto Portugûes do mar e da Atmosfera), n.d. Normais Climatologicas 1971-2000 [WWW Document]. URL https://www.ipma.pt/pt/oclima/normais.clima/1971-2000/#535 (accessed 8.3.21).

Jarvis, P., Rey, A., Petsikos, C., Wingate, L., Rayment, M., Pereira, J., Banza, J., David, J., Miglietta, F., Borghetti, M., Manca, G., Valentini, R., 2007. Drying and wetting of Mediterranean soils stimulates decomposition and carbon dioxide emission: the "Birch effect" Tree Physiol. 27, 929–940. https://doi.org/10.1093/treephys/27.7.929

Jongen, M., Lecomte, X., Unger, S., Fangueiro, D., Pereira, J.S., 2013. Precipitation variability does not affect soil respiration and nitrogen dynamics in the understorey of a Mediterranean oak woodland. Plant Soil 372, 235–251. https://doi.org/10.1007/s11104-013-1728-7

Jongen, M., Pereira, J.S., Aires, L.M.I., Pio, C.A., 2011. The effects of drought and timing of precipitation on the inter-annual variation in ecosystem-atmosphere exchange in a Mediterranean grassland. Agric. For. Meteorol. 151, 595–606. https://doi.org/10.1016/j.agrformet.2011.01.008

Jönsson, P., Eklundh, L., 2004. TIMESAT—a program for analyzing time-series of satellite sensor data. Comput. Geosci. 30, 833–845. https://doi.org/https://doi.org/10.1016/j.cageo.2004.05.006

Jönsson, P., Eklundh, L., 2002. Seasonality extraction by function fitting to time-series of satellite sensor data. IEEE Trans. Geosci. Remote Sens. 40, 1824–1832.

https://doi.org/10.1109/TGRS.2002.802519

Jung, M., Reichstein, M., Schwalm, C.R., Huntingford, C., Sitch, S., Ahlström, A., Arneth, A., Camps-Valls, G., Ciais, P., Friedlingstein, P., Gans, F., Ichii, K., Jain, A.K., Kato, E., Papale, D., Poulter, B., Raduly, B., Rödenbeck, C., Tramontana, G., Viovy, N., Wang, Y.-P., Weber, U., Zaehle, S., Zeng, N., 2017. Compensatory water effects link yearly global land CO2 sink changes to temperature. Nature 541, 516–520. https://doi.org/10.1038/nature20780

Kljun, N., Calanca, P., Rotach, M.W., Schmid, H.P., 2015. A simple two-dimensional parameterisation for Flux Footprint Prediction (FFP). Geosci. Model Dev. 8, 3695–3713. https://doi.org/10.5194/gmd-8-3695-2015

Liu, Y., Schwalm, C.R., Samuels-Crow, K.E., Ogle, K., 2019. Ecological memory of daily carbon exchange across the globe and its importance in drylands. Ecol. Lett. 22, 1806–1816. https://doi.org/10.1111/ele.13363

Luo, Y., El-Madany, T.S., Filippa, G., Ma, X., Ahrens, B., Carrara, A., Gonzalez-Cascon, R., Cremonese, E., Galvagno, M., Hammer, T.W., Pacheco-Labrador, J., Martín, M.P., Moreno, G., Perez-Priego, O., Reichstein, M., Richardson, A.D., Römermann, C., Migliavacca, M., Luo, Y., El-Madany, T.S., Filippa, G., Ma, X., Ahrens, B., Carrara, A., Gonzalez-Cascon, R., Cremonese, E., Galvagno, M., Hammer, T.W., Pacheco-Labrador, J., Martín, M.P., Moreno, G., Perez-Priego, O., Reichstein, M., Richardson, A.D., Römermann, C., Migliavacca, M., 2018. Using Near-Infrared-Enabled Digital Repeat Photography to Track Structural and Physiological Phenology in Mediterranean Tree–Grass Ecosystems. Remote Sens. 10, 1293. https://doi.org/10.3390/rs10081293

Luo, Y., El-Madany, T., Ma, X., Nair, R., Jung, M., Weber, U., Filippa, G., Bucher, S.F., Moreno, G., Cremonese, E., Carrara, A., Gonzalez-Cascon, R., Cáceres Escudero, Y., Galvagno, M., Pacheco-Labrador, J., Martín, M.P., Perez-Priego, O., Reichstein, M., Richardson, A.D., Menzel, A., Römermann, C., Migliavacca, M., 2020. Nutrients and water availability constrain the seasonality of vegetation activity in a Mediterranean ecosystem. Glob. Chang. Biol. gcb.15138. https://doi.org/10.1111/gcb.15138

757 Ma, S., Baldocchi, D., Wolf, S., Verfaillie, J., 2016. Slow ecosystem responses conditionally
758 regulate annual carbon balance over 15 years in Californian oak-grass savanna. Agric. For.
759 Meteorol. 228–229, 252–264. https://doi.org/10.1016/J.AGRFORMET.2016.07.016
760 Ma, S., Baldocchi, D.D., Xu, L., Hehn, T., 2007. Inter-annual variability in carbon dioxide
761 exchange of an oak/grass savanna and open grassland in California. Agric. For. Meteorol.
762 147, 157–171. https://doi.org/10.1016/J.AGRFORMET.2007.07.008
763 Ma, X., Mahecha, M.D., Migliavacca, M., van der Plas, F., Benavides, R., Ratcliffe, S., Kattge,
764 J., Richter, R., Musavi, T., Baeten, L., Barnoaiea, I., Bohn, F.J., Bouriaud, O., Bussotti, F.,
765 Coppi, A., Domisch, T., Huth, A., Jaroszewicz, B., Joswig, J., Pabon-Moreno, D.E.,
766 Papale, D., Selvi, F., Laurin, G.V., Valladares, F., Reichstein, M., Wirth, C., 2019.
767 Inferring plant functional diversity from space: the potential of Sentinel-2. Remote Sens.
768 Environ. 233, 111368. https://doi.org/10.1016/J.RSE.2019.111368
769 Manabe, S., 1969. Climate and the ocean circulation,1. The atmospheric circulation and the
770 hydrologyof the earth's surface. Mon. Wea. Rev. 97, 739–774.
771 Marchin, R.M., McHugh, I., Simpson, R.R., Ingram, L.J., Balas, D.S., Evans, B.J., Adams,
772 M.A., 2018. Productivity of an Australian mountain grassland is limited by temperature
773 and dryness despite long growing seasons. Agric. For. Meteorol. 256–257, 116–124.
774 https://doi.org/10.1016/J.AGRFORMET.2018.02.030
775 Marcolla, B., Cescatti, A., Manca, G., Zorer, R., Cavagna, M., Fiora, A., Gianelle, D.,
776 Rodeghiero, M., Sottocornola, M., Zampedri, R., 2011. Climatic controls and ecosystem
777 responses drive the inter-annual variability of the net ecosystem exchange of an alpine
778 meadow. Agric. For. Meteorol. 151, 1233–1243.
779 https://doi.org/10.1016/J.AGRFORMET.2011.04.015
780 Migliavacca, M., Reichstein, M., Richardson, A.D., Colombo, R., Sutton, M.A., Lasslop, G.,
781 Tomelleri, E., Wohlfahrt, G., Carvalhais, N., Cescatti, A., Mahecha, M.D., Montagnani,
782 L., Papale, D., Zaehle, S., Arain, A., Arneth, A., Black, T.A., Carrara, A., Dore, S.,
783 Gianelle, D., Helfter, C., Hollinger, D., Kutsch, W.L., Lafleur, P.M., Nouvellon, Y.,
784 Rebmann, C., Humberto, R., Rodeghiero, M., Roupsard, O., Sebastià, M.T., Seufert, G.,

785 Soussana, J.F., Van Der Molen, M.K., 2011. Semiempirical modeling of abiotic and biotic
786 factors controlling ecosystem respiration across eddy covariance sites. Glob. Chang. Biol.
787 17, 390–409. https://doi.org/10.1111/j.1365-2486.2010.02243.x
788 Migliavacca, M., Reichstein, M., Richardson, A.D., Mahecha, M.D., Cremonese, E., Delpierre,
789 N., Galvagno, M., Law, B.E., Wohlfahrt, G., Andrew Black, T., Carvalhais, N.,
790 Ceccherini, G., Chen, J., Gobron, N., Koffi, E., William Munger, J., Perez-Priego, O.,
791 Robustelli, M., Tomelleri, E., Cescatti, A., 2015. Influence of physiological phenology on
792 the seasonal pattern of ecosystem respiration in deciduous forests. Glob. Chang. Biol. 21,
793 363–376. https://doi.org/10.1111/gcb.12671
794 Mori, A.S., Lertzman, K.P., Gustafsson, L., 2017. Biodiversity and ecosystem services in forest
795 ecosystems: a research agenda for applied forest ecology. J. Appl. Ecol. 54, 12–27.
796 https://doi.org/10.1111/1365-2664.12669
797 Musavi, T., Migliavacca, M., Reichstein, M., Kattge, J., Wirth, C., Black, T.A., Janssens, I.,
798 Knohl, A., Loustau, D., Roupsard, O., Varlagin, A., Rambal, S., Cescatti, A., Gianelle, D.,
799 Kondo, H., Tamrakar, R., Mahecha, M.D., 2017. Stand age and species richness dampen
800 interannual variation of ecosystem-level photosynthetic capacity. Nat. Ecol. Evol. 1, 1–7.
801 https://doi.org/10.1038/s41559-016-0048
802 Nogueira, C., Bugalho, M.N., Pereira, J.S., Caldeira, M.C., 2017. Extended autumn drought, but
803 not nitrogen deposition, affects the diversity and productivity of a Mediterranean
804 grassland. Environ. Exp. Bot. 138, 99–108.
805 https://doi.org/10.1016/j.envexpbot.2017.03.005
806 Papale, D., Reichstein, M., Aubinet, M., Canfora, E., Bernhofer, C., Kutsch, W., Longdoz, B.,
807 Rambal, S., Valentini, R., Vesala, T., Yakir, D., 2006. Towards a standardized processing
808 of Net Ecosystem Exchange measured with eddy covariance technique: algorithms and
809 uncertainty estimation. Biogeosciences 3, 571–583. https://doi.org/10.5194/bg-3-571-2006
810 Pereira, J.S., Mateus, J.A., Aires, L.M., Pita, G., Pio, C., David, J.S., Banza, J., David, T.S.,
811 Paço, T. a., Pereira, J.S., Mateus, J.A., Aires, L.M., Pita, G., Pio, C., Andrade, V., Banza,
812 J., David, T.S., Paço, T. a., Rodrigues, A., 2007. Net ecosystem carbon exchange in three

contrasting Mediterranean ecosystems – the effect of drought. Biogeosciences 4, 791–802. https://doi.org/10.5194/bg-4-791-2007

Piayda, A., Dubbert, M., Rebmann, C., Kolle, O., Costa e Silva, F., Correia, A., Pereira, J.S., Werner, C., Cuntz, M., 2014. Drought impact on carbon and water cycling in a Mediterranean <i>Quercus suber</i> L. woodland during the extreme drought event in 2012. Biogeosciences 11, 7159–7178. https://doi.org/10.5194/bg-11-7159-2014

Pinto, C.A., Nadezhdina, N., David, J.S., Kurz-Besson, C., Caldeira, M.C., Henriques, M.O., Monteiro, F.G., Pereira, J.S., David, T.S., 2014. Transpiration in *Quercus suber* trees under shallow water table conditions: the role of soil and groundwater. Hydrol. Process. 28, 6067–6079. https://doi.org/10.1002/hyp.10097

Poulter, B., Frank, D., Ciais, P., Myneni, R.B., Andela, N., Bi, J., Broquet, G., Canadell, J.G., Chevallier, F., Liu, Y.Y., Running, S.W., Sitch, S., van der Werf, G.R., 2014. Contribution of semi-arid ecosystems to interannual variability of the global carbon cycle. Nature 509, 600+. https://doi.org/10.1038/nature13376

R CoreTeam, 2016. No Title. R A Lang. Environ. Stat. Comput.

Reichstein, M., Bahn, M., Ciais, P., Frank, D., Mahecha, M.D., Seneviratne, S.I., Zscheischler, J., Beer, C., Buchmann, N., Frank, D.C., Papale, D., Rammig, A., Smith, P., Thonicke, K., van der Velde, M., Vicca, S., Walz, A., Wattenbach, M., 2013. Climate extremes and the carbon cycle. Nature 500, 287–295. https://doi.org/10.1038/nature12350

Reichstein, M., Falge, E., Baldocchi, D., Papale, D., Aubinet, M., Berbigier, P., Bernhofer, C., Buchmann, N., Gilmanov, T., Granier, A., Grunwald, T., Havrankova, K., Ilvesniemi, H., Janous, D., Knohl, A., Laurila, T., Lohila, A., Loustau, D., Matteucci, G., Meyers, T., Miglietta, F., Ourcival, J.-M., Pumpanen, J., Rambal, S., Rotenberg, E., Sanz, M., Tenhunen, J., Seufert, G., Vaccari, F., Vesala, T., Yakir, D., Valentini, R., 2005. On the separation of net ecosystem exchange into assimilation and ecosystem respiration: review and improved algorithm. Glob. Chang. Biol. 11, 1424–1439. https://doi.org/10.1111/j.1365-2486.2005.001002.x

Reichstein, M., Papale, D., Valentini, R., Aubinet, M., Bernhofer, C., Knohl, A., Laurila, T.,

Lindroth, A., Moors, E., Pilegaard, K., Seufert, G., 2007. Determinants of terrestrial ecosystem carbon balance inferred from European eddy covariance flux sites. Geophys. Res. Lett. 34, L01402. https://doi.org/10.1029/2006GL027880

Reichstein, M., Tenhunen, J.D., Roupsard, O., Ourcival, J., Rambal, S., Miglietta, F., Peressotti, A., Pecchiari, M., Tirone, G., Valentini, R., 2002. Severe drought effects on ecosystem CO2 and H2O fluxes at three Mediterranean evergreen sites: revision of current hypotheses? Glob. Chang. Biol. 8, 999–1017. https://doi.org/10.1046/j.1365-2486.2002.00530.x

Richardson, A.D., Andy Black, T., Ciais, P., Delbart, N., Friedl, M.A., Gobron, N., Hollinger, D.Y., Kutsch, W.L., Longdoz, B., Luyssaert, S., Migliavacca, M., Montagnani, L., William Munger, J., Moors, E., Piao, S., Rebmann, C., Reichstein, M., Saigusa, N., Tomelleri, E., Vargas, R., Varlagin, A., 2010. Influence of spring and autumn phenological transitions on forest ecosystem productivity. Philos. Trans. R. Soc. B Biol. Sci. 365, 3227–3246. https://doi.org/10.1098/rstb.2010.0102

RICHARDSON, A.D., HOLLINGER, D.Y., ABER, J.D., OLLINGER, S. V., BRASWELL, B.H., 2007. Environmental variation is directly responsible for short- but not long-term variation in forest-atmosphere carbon exchange. Glob. Chang. Biol. 13, 788–803. https://doi.org/10.1111/j.1365-2486.2007.01330.x

Ross, I., Misson, L., Rambal, S., Arneth, A., Scott, R.L., Carrara, A., Cescatti, A., Genesio, L., 2012. How do variations in the temporal distribution of rainfall events affect ecosystem fluxes in seasonally water-limited Northern Hemisphere shrublands and forests? Biogeosciences 9, 1007–1024. https://doi.org/10.5194/bg-9-1007-2012

Savitzky, A., Golay, M.J.E., 1964. Smoothing and Differentation of Data by Simplified least squares Procedures. Anal. Chem. 1627–1639.

Schaaf, C.B., Wang, Z., 2015a. MCD43A4 MODIS/Terra+Aqua BRDF/Albedo Nadir BRDF Adjusted Ref Daily L3 Global [WWW Document]. NASA EOSDIS L. Process. DAAC. URL https://doi.org/https://doi.org/10.5067/MODIS/MCD43A4.006

Schaaf, C.B., Wang, Z., 2015b.

MCD43A2MODIS/Terra+AquaBRDF/AlbedoQualityDailyL3Global-500mV006 [WWW Document]. NASA EOSDIS L. Process. DAAC. URL https://doi.org/https://doi.org/10.5067/MODIS/MCD43A2.006

Seneviratne, S.I., Corti, T., Davin, E.L., Hirschi, M., Jaeger, E.B., Lehner, I., Orlowsky, B., Teuling, A.J., 2010. Investigating soil moisture–climate interactions in a changing climate: A review. Earth-Science Rev. 99, 125–161. https://doi.org/10.1016/j.earscirev.2010.02.004

Soares, C., Silva, J.M.N., Boavida-Portugal, J., Cerasoli, S., 2022. Spectral-Based Monitoring of Climate Effects on the Inter-Annual Variability of Different Plant Functional Types in Mediterranean Cork Oak Woodlands. Remote Sens. 14, 711. https://doi.org/10.3390/rs14030711

Tucker, C.J., 1979. Red and Photographic Infrared Linear Combinations for Monitoring Vegetation. Remote Sens. Environ. 8, 127–150.

Vickers, D., Mahrt, L., 1997. Quality control anf lux sampling problems for tower and aircraft data. J. Atmos. Ocean. Technol. 14, 512–526.

Wang, J., Dong, J., Liu, J., Huang, M., Li, G., Running, S., Smith, W., Harris, W., Saigusa, N., Kondo, H., Liu, Y., Hirano, T., Xiao, X., 2014. Comparison of Gross Primary Productivity Derived from GIMMS NDVI3g, GIMMS, and MODIS in Southeast Asia. Remote Sens. 6, 2108–2133. https://doi.org/10.3390/rs6032108

Wilczak, J.M., Oncley, S.P., Stage, S.A., 2001. Sonic anemometer tilt correction algorithms. Boundary-Layer Meteorol. 99, 127–150. https://doi.org/10.1023/A:1018966204465

Wutzler, T., Lucas-Moffat, A., Migliavacca, M., Knauer, J., Sickel, K., Šigut, L., Menzer, O., Reichstein, M., 2018. Basic and extensible post-processing of eddy covariance flux data with REddyProc. Biogeosciences 15, 5015–5030. https://doi.org/10.5194/bg-15-5015-2018

Zhang, T., Xu, M., Xi, Y., Zhu, J., Tian, L., Zhang, X., Wang, Y., Li, Y., Shi, P., Yu, G., Sun, X., Zhang, Y., 2015. lagged climatic effects on carbon fluxes over three grassland ecosystems in China. J. Plant Ecol. 8, 291–302. https://doi.org/10.1093/jpe/rtu026

Zscheischler, J., Reichstein, M., von Buttlar, J., Mu, M., Randerson, J.T., Mahecha, M.D., 2014. Carbon cycle extremes during the 21st century in CMIP5 models: Future evolution and attribution to climatic drivers. Geophys. Res. Lett. 41, 8853–8861. https://doi.org/10.1002/2014GL062409